Phonoionization of A^+ states in Si under uniaxial stress: Influence of the valence-band structure

R. Haug and E. Sigmund
Institut für Theoretische Physik, Universität Stuttgart, Pfaffenwaldring 57, D-7000 Stuttgart 80, Federal Republic of Germany
(Received 16 February 1988; revised manuscript received 8 March 1989)

Scattering of phonons at shallow bound A^+ states in Si can lead to a neutralization of these states and simultaneously to an increase of mobile charge carriers in the valence band, which causes an increase of the electrical conductivity. We investigate the coupling of phonons to A^+ states in Si and calculate the phonon-induced conductivity in dependence of the phonon energy. The calculations are based on a Kubo-Mori formalism. Uniaxial stress decouples degenerate valence bands and causes a mixing of spin-orbit-split valence bands leading to a change of the valence-band structure and to striking effects on the phonoconductivity. These effects described in the theory have been observed experimentally.

I. INTRODUCTION

Shallow impurities in semiconductors at low temperatures can bind a second carrier to form H^--like states. Then phonon scattering at these states can create mobile charge carriers through excitation. This induces a change in the electrical conductivity which can be used as detecting mechanism. An estimate of the binding energies of D^- states of donors and A^+ states of acceptors can be obtained from thresholds in far-infrared (FIR) photoconductivity and phonon spectroscopy. Both experiments lead to the same threshold energies, e.g., in the case of B^+ or P^- in Si and thereby prove that the neutralization by phonons is mainly a one-phonon process[1–3].

Since the wavelengths of the phonons which interact most strongly with the defect states are comparable to the extent of these states the coupling of phonons to D^- and A^+ centers, and thus the phonon-induced conductivity strongly depends on the energy of the phonons. In addition, the wave vector of the state of the mobile charge carrier and the corresponding effective mass have a great influence on the phonoconductivity. This can be demonstrated by applying uniaxial stress which, especially in the case of A^+ states, leads to great influence on the phonoconductivity.

In this paper we study the scattering of phonons at A^+ states in Si. By means of phonon spectroscopy the binding energies of A^+ states in Si have been found to be about 1.8 meV for B^+, Al^+, and Ga^+, and 5.9 meV for In^+.[4] The neutralization of these states by phonons leads to an increased electrical conductivity, which is called *phono*conductivity, in contrast to the *photo*conductivity where the mobile charge carriers are created by optical methods. In Sec. II A the wave functions for A^+ centers in Si based on the effective-mass approximation are discussed. Further on, the Hamiltonian for the electron-phonon interactions is derived. In Secs. II B–II E we investigate the influence of uniaxial stress on the phonoconductivity. It turns out that externally applied stress leads to a splitting of the A^+ state as well as of the valence-band states. Additionally, we show the stress-dependent mixing and coupling of the valence bands and their influence on the electrical conductivity. In Sec. II F matrix elements are calculated describing the dependence of the electron-phonon interaction on the phonon energy. Then, in Sec. II G we develop a microscopic single-particle theory which allows us to calculate the phonon-induced electrical conductivity starting from the Kubo formula[5] and applying the Mori formalism.[6] Finally, in Sec. III the results are presented and compared with experimental measurements.

II. THEORY

The top of the valence band in Si is at the center of the Brillouin zone (at the Γ point) and has sixfold degeneracy, resulting from a threefold orbital ($L=1$) and a twofold spin degeneracy ($S=\frac{1}{2}$). Spin-orbit interaction partially splits these degeneracies, leading to a higher-lying quadruplet ($J=\frac{3}{2}$) and a lower-lying doublet ($J=\frac{1}{2}$) state. This structure is reflected in the bound states of shallow-acceptor impurities, which in an effective-mass approximation can be represented by wave packets made up largely of the six Bloch waves chosen from the top of the valence band with appropriate envelope functions describing the localization of the defect. The envelope functions are equivalents to the hydrogenic eigenfunctions and can be calculated by solving the set of effective-mass equations.[7] For this the envelope functions are expanded in spherical harmonics characterized by the quantum numbers l and m. The effective-mass equations have inversion symmetry, and therefore either even-l or odd-l terms contribute to the solution only. Since the ground-state wave functions are mainly s-like ($l=0$), the even-l expansion is chosen. In the following we consider the $l=0$ (s-like) and $l=2$ (d-like) contributions only.

The A^+ state is fourfold degenerate due to the

tetrahedral symmetry of the surrounding crystal. We neglect correlation effects of the two holes bound by the acceptor. This is justified since the hole-hole coupling would lead to a multiplet structure, which, however, has not yet been found in measurements of the A^+ binding energies in Si.[4] Therefore, as the wave function for the second hole we can adopt the form of the wave function of the acceptor–ground-state quartet ($J=\frac{3}{2}$), specified by $M_J=\frac{3}{2}, \frac{1}{2}, -\frac{1}{2}$, and $-\frac{3}{2}$.

This function has been determined by Suzuki, Okazaki, and Hasegawa,[8] within the framework of the effective-mass approximation. Including s- and d-like envelope parts, they used a variational procedure to calculate the explicit structure of the wave functions Ψ^{M_J} of the acceptor–ground-state quartet. Each wave function can be represented as a linear combination of six orthogonal component vectors $\Phi_i^{M_J}$, whereby one of these includes only s-like terms, and the remaining five have only d-like character. Thus the wave function can be written as

$$\Psi^{M_J}=\sum_{i=0}^{5} C_i \Phi_i^{M_J} , \tag{2.1}$$

where in a first step of the variational procedure the coefficients C_i have been determined, and then in a second one the corresponding effective Bohr radii describe the extent of the wave function.[8] We approximate the wave function of the second hole by the single-particle function of Suzuki *et al.* with effective Bohr radii of about 1.5 times the values of the neutral-acceptor states. The expression for the wave function $\Phi_i^{M_J}$ is derived for the axis of quantization along [001]. Fjeldly *et al.*[7] worked out the corresponding expression for the axis of quantization along [111].

The strain Hamiltonian describing the coupling of phonons to the A^+ state and the splitting of the ground-state quartet by external stress can be derived from symmetry considerations:[9]

$$H_I^v=D_d^v(e_{xx}+e_{yy}+e_{zz})+2D_u[(L_x^2-\tfrac{1}{3}L^2)e_{xx}+\text{c.p.}] +D_{u'}[(L_xL_y+L_yL_x)e_{xy}+\text{c.p.}] , \tag{2.2}$$

where L_α is the α component of the angular-momentum operator $\mathbf{L}$ ($L=1$). $\alpha=x$, y, or z refers to the fourfold-symmetry axes. D_d^v, D_u, and $D_{u'}$ are the valence-band deformation-potential constants. c.p. denotes cyclic permutation of the indices x, y, and z. $e_{\alpha\beta}$ are the conventional strain components.[9] The coupling of the totally symmetric part of the elastic distortion is neglected, since it yields only a constant energy shift without splitting of the ground state. D_u and $D_{u'}$ define the valence-band splitting for uniaxial stress along the [001] and [111] directions, respectively.

The strain Hamiltonian (2.2) describes the splitting of the energy in the A^+ state quartet caused by static strain and the coupling of the A^+ state to phonons. In both cases the Hamiltonian operates on the A^+ wave function (2.1). The calculations can now be carried out by representing H_I^v as a 6×6 matrix within the same basis we used to build up Ψ^{M_J}.[7] It is convenient to choose the direction of the external stress as the axis of quantization. Thus, for uniaxial stress along [001], α corresponds to x, y, and z of Eq. (2.2). In the case of [111] stress, α refers to the axes of a coordinate system with the z' axes ($\alpha=3$) along the [111] direction. The x' and y' axes are chosen along the $[1\bar{1}0]$ and $[11\bar{2}]$, respectively. L_x, L_y, and L_z must then be decomposed along the new coordinate axes.[7]

A. Stress-induced energy splitting

For stress along a threefold- or fourfold-symmetry axis, the A^+ quartet splits into two doublets, $M_J=\pm\frac{3}{2}$ and $\pm\frac{1}{2}$, with an energy separation Δ. In the case of a cubic system with uniaxial stress X along the [001] direction, the elastic-strain components are

$$\begin{aligned} e_{xx}&=e_{yy}=S_{12}X , \\ e_{zz}&=S_{11}X , \\ e_{xy}&=e_{xz}=e_{yz}=0 , \end{aligned} \tag{2.3}$$

and for the [111] stress direction, they read

$$\begin{aligned} e_{xx}&=e_{yy}=e_{zz}=\tfrac{1}{3}(S_{11}+2S_{12})X , \\ e_{xy}&=e_{xz}=e_{zy}=\tfrac{1}{3}S_{44}X , \end{aligned} \tag{2.4}$$

where S_{11}, S_{12}, and S_{44} are the cubic-compliance constants.

The separation Δ of the two Kramers doublets for stress along [001] is

$$\Delta=\tfrac{4}{3}D_u^A(S_{11}-S_{12})X , \tag{2.5}$$

and for stress along [111],

$$\Delta=\tfrac{2}{3}D_{u'}^A S_{44}X . \tag{2.6}$$

D_u^A and $D_{u'}^A$ are the A^+-state deformation-potential constants depending on the coefficients C_i of the wave function (2.1).[7]

B. Valence-band structure in the presence of strain

In the absence of stress the interaction between the degenerate valence bands at $k=0$ disturbs the energy surfaces and leads to quartic terms in the wave-vector expansion. These warped surfaces are described in terms of inverse-mass band parameters. A, B, and N.[10] Uniaxial stress lifts the cubic symmetry of the crystal and removes the degeneracy at $k=0$. For stress along the [001] and [111] directions the decoupled states are degenerate Kramers's doublets identified by the quantum number $\pm M_J$. In the case that the applied stress is strong enough to decouple the two bands with $J=\frac{3}{2}$ completely, their energy surfaces are ellipsoidal.[10]

Without strain the energy surfaces for the $J=\frac{3}{2}$ band are

$$E(k)=Ak^2\pm[B^2k^4+C^2(k_x^2k_y^2+k_x^2k_z^2+k_y^2k_z^2)]^{1/2} , \tag{2.7}$$

where C again is an inverse band parameter depending on N and B.[10] The plus and minus signs in (2.7) refer to

heavy and light holes, respectively. The $J=\frac{1}{2}$ band has spherical energy surfaces given by

$$E(k)=Ak^2-\Lambda\ , \tag{2.8}$$

with the energy lowering $\Lambda=0.044$ eV caused by spin-orbit interaction.

For stress along [001] the eigenvalues of the Hamiltonian describing the valence-band states are to lowest order in k,

$$E_{3/2}(k)=(A+\tfrac{1}{2}B)k_\perp^2+(A-B)k_\parallel^2+\varepsilon/2 \tag{2.9}$$

and

$$E_{1/2}(k)=(A-\tfrac{1}{2}B)k_\perp^2+(A+B)k_\parallel^2-\varepsilon/2\ , \tag{2.10}$$

where

$$k_\perp^2=k_x^2+k_y^2 \quad \text{and} \quad k_\parallel^2=k_z^2\ . \tag{2.11}$$

ε is the energy separation between the two Kramers's doublets and is obtained from (2.5) by replacing D_u^A by D_u. Thus, the energy surfaces near $k=0$ become ellipsoids with axis of symmetry along the stress direction. For stress along [111] the eigenvalues to lowest order of k are

$$E_{3/2}(k)=(A+\tfrac{1}{6}N)k_\perp^2+(A-\tfrac{1}{3}N)k_\parallel^2+\varepsilon'/2 \tag{2.12}$$

and

$$E_{1/2}(k)=(A-\tfrac{1}{6}N)k_\perp^2+(A+\tfrac{1}{3}N)k_\parallel^2-\varepsilon'/2\ , \tag{2.13}$$

where

$$k_\perp^2=k_1^2+k_2^2 \quad \text{and} \quad k_\parallel^2=k_3^2\ . \tag{2.14}$$

The splitting ε' can be obtained from Eq. (2.6) by replacing $D_{u'}^A$ by $D_{u'}$. Again the energy surfaces are ellipsoids.[10]

C. Linear mass shift due to valence-band mixing

The existence of the degeneracy with $J=\frac{3}{2}$ in the case of $X=0$ is a consequence of the spherical isotropy of the spin-orbit interaction.[9] This isotropy is violated by uniaxial stress, resulting in a splitting of the terms and a mixing of the eigenstates of $J=\frac{3}{2}$ with $J=\frac{1}{2}$. Since M_J is still a good quantum number under uniaxial stress, the mixing takes place only between the two doublets with $M_J=\pm\frac{1}{2}$. The degree of mixing depends on the relative strength of the strain energy ε or ε' to the spin-orbit separation Λ.[9] If one calculates the energy bands by omitting the off-diagonal elements of the Hamiltonian for the valence-band states, the energy surfaces described in the preceding subsection are obtained. When including the off-diagonal elements, and thus taking into account the admixture of the spin-orbit-split-off state ($J=\frac{1}{2}$), Eqs. (2.10) and (2.13) are modified and read

$$E_{1/2}(k)=[A-\tfrac{1}{2}B(1-2\varepsilon/\Lambda)]k_\perp^2 +[A+B(1-2\varepsilon/\Lambda)]k_\parallel^2-\varepsilon/2 \tag{2.15}$$

for stress along [001], and

$$E_{1/2}(k)=[A-\tfrac{1}{6}N(1-2\varepsilon'/\Lambda)]k_\perp^2 +[A+\tfrac{1}{3}N(1-2\varepsilon'/\Lambda)]k_\parallel^2-\varepsilon'/2 \tag{2.16}$$

for stress along the [111] direction, while Eqs. (2.9) and (2.12) remain unchanged.[9] In low order the inverse effective mass of the states with $M_J=\pm\frac{1}{2}$ depends linearly on the stress.

D. Effects of fourth-order terms

Second-order perturbation theory leads to a correction of the energy surfaces discussed in the preceding two subsections that is given by fourth-order terms in the three variables k_x, k_y, and k_z. These terms are important when the applied stress is not strong enough to decouple the upper two valence bands completely. In this case their nonparabolic structure becomes significant. The second-order perturbation-energy correction for the band with $J=\frac{3}{2}$ and $M_J=\frac{1}{2}$ is given by[9]

$$\Delta E_{1/2}=(1/\varepsilon)(|U|^2+|V|^2)\ . \tag{2.17}$$

For the case of applied stress along [001], U and V are

$$U=\frac{1}{\sqrt{3}}Nk_z(k_x+ik_y) \tag{2.18}$$

and

$$V=\frac{\sqrt{3}}{2}B(k_x^2-k_y^2)+\frac{i}{\sqrt{3}}Nk_xk_y\ . \tag{2.19}$$

For stress along [111], U and V are given by

$$U=-\frac{1}{\sqrt{6}}(B-N/3)(k_1-ik_2)^2 +\frac{1}{\sqrt{3}}(2B+N/3)k_3(k_1+ik_2) \tag{2.20}$$

and

$$V=-\frac{1}{\sqrt{3}}(B/2+N/3)(k_1+ik_2)^2 -(\tfrac{2}{3})^{1/2}(B-N/3)k_3(k_1-ik_2)\ , \tag{2.21}$$

where the coordinates (1,2,3) are chosen so that 3 is parallel to the stress axis [111]. 1 and 2 are along the $[11\bar{2}]$ and $[\bar{1}10]$ axes, respectively. This second-order correction for the energy always leads to an increased effective mass and is directly proportional to the applied uniaxial stress.

E. Phonon matrix elements

For the description of the dynamics of the system, the coupling of the A^+ state to acoustic phonons has to be considered instead of the coupling to static deformations discussed in Sec. II A. The elastic constants $e_{\alpha\beta}$ can be expressed by the displacement vectors $\mathbf{u}$ of the atoms by

$$e_{\alpha\beta}-\frac{1}{2}\left[\frac{\partial \mathbf{u}_\alpha}{\partial\beta}+\frac{\partial \mathbf{u}_\beta}{\partial\alpha}\right] \quad (\alpha,\beta=x,y,z)\ . \tag{2.22}$$

The displacement $\mathbf{u}$ can be expanded in terms of the vi-

brational modes of the crystal. This leads to

$$\mathbf{u}(\mathbf{r})=\sum_{\mathbf{q},\lambda}\left[\frac{\hbar}{2M\omega_{\mathbf{q}\lambda}}\right]^{1/2}\mathbf{e}_{\mathbf{q}\lambda}[\exp(i\mathbf{q}\cdot\mathbf{r})b_{\mathbf{q}\lambda}+\exp(-i\mathbf{q}\cdot\mathbf{r})b^{\dagger}_{\mathbf{q}\lambda}] . \tag{2.23}$$

$b_{\mathbf{q}\lambda}$ and $b^{\dagger}_{\mathbf{q}\lambda}$ are the annihilation and creation operators for the phonon with wave vector $\mathbf{q}$ in the branch λ, $\omega_{\mathbf{q}\lambda}$ is the angular frequency, and $\mathbf{e}_{\mathbf{q}\lambda}$ is the polarization vector of the phonon. M is the mass of the crystal. Here the long-wavelength approximation for the phonon dispersion is used,

$$\omega_{\mathbf{q}\lambda}=c_{\mathbf{q}\lambda}|\mathbf{q}| . \tag{2.24}$$

The matrix elements describing the phonon-induced coupling between the stress-split doublets of the A^+ state and the valence-band states are obtained by substituting the expansion in normal modes for the strain components (2.22) and (2.23) into the strain Hamiltonian (2.2). We use the wave function as discussed in Sec. II for the A^+ state and Bloch waves in the same representation for the valence-band states. The axis of quantization is chosen along the direction of uniaxial stress.

The matrix elements contain integrals over the space variables that consist of products between the various s- and d-like angular parts of the A^+ state (Ref. 7), their radial parts, a phase factor $e^{i\mathbf{q}\cdot\mathbf{r}}$ from the expansion of the strain components into normal modes, and a factor $e^{i\mathbf{k}\cdot\mathbf{r}}$ from the Bloch function of the valence-band state. These integrals are rather complicated, but assuming that $|\mathbf{k}|\ll|\mathbf{q}|$ the integrations can be performed analytically. As a result, one is left with only two form factors, which appear in different linear combinations in the matrix elements for the various transitions between the states of the A^+ quartet and the upper valence bands. The s-like part of the A^+ state gives a form factor f_0 which reads

$$f_0=(1+r_1^2q^2)^{-2} , \tag{2.25}$$

and the d-like part

$$f_2=r_2^2q^2(1+r_2^2q^2)^{-4} . \tag{2.26}$$

r_1 and r_2 are the effective Bohr radii for the s- and d-like parts, respectively. These form factors reflect the strong dependence of the electron-phonon interaction on the phonon energy since the wave lengths of the phonons that are important for the scattering process are comparable to the effective Bohr radii.

As a result, the matrix elements M can then be written as sums of products between the amplitude factors C_i and the form factors f_0 and f_2,

$$M_{M_J^VM_J^A}=\langle M_J^V|H_I^V|M_J^A\rangle=\sum_{\mathbf{q},\lambda}\left[\frac{\hbar\omega_{q\lambda}}{2Mc_\lambda^2}\right]^{1/2}C_{\mathbf{q}\lambda}^{M_J^VM_J^A}(b_{\mathbf{q}\lambda}+b^{\dagger}_{\mathbf{q}\lambda}) . \tag{2.27}$$

The coupling constants $C_{\mathbf{q}\lambda}^{M_J^VM_J^A}$ are given by

$$C_{\mathbf{q}\lambda}^{M_J^VM_J^A}=D_u\sum_{i=0}^{5}\alpha_{i\lambda}^{M_J^VM_J^A}C_if^i+D_{u'}\sum_{i=0}^{5}\beta_{i\lambda}^{M_J^VM_J^A}C_if^i . \tag{2.28}$$

The α_i and β_i are complex numbers and $f^i=f_0$ for $i=0$ and $f^i=f_2$ for $i\neq0$. $|M_J^V\rangle$ is the valence-band state and $|M_J^A\rangle=|\Psi^{M_J}\rangle$ is the A^+ wave function (2.1) with $J=\frac{3}{2}$, respectively. We have calculated the explicit expressions for the coupling constants for two cases of configurations with different stress and phonon-propagation directions: (i) uniaxial stress along [001] with $\mathbf{q}\|[100]$, and (ii) stress along [111] with $\mathbf{q}\|[1\bar{1}0]$. In order to obtain analytic expressions, a quasi-isotropic model for the elastic properties of the crystal has been adopted.[7] This results in simple expressions for the polarization vectors $\mathbf{e}_{\mathbf{q}\lambda}$ for the three acoustical modes.

F. Phonoconductivity

Phonons with energy greater than the binding energy of an A^+ state can neutralize this state and create mobile charge carriers, which causes an increase of the electrical conductivity. We use the Kubo formula[5] to derive an expression for the phonon-induced change of conductivity by means of Mori's formalism.[6] Within this formalism, the model can easily be extended in order to describe concentration- and temperature-dependent effects. Although we do not discuss these dependencies in this context, we want to give here already a short description of the more general theory.

We want to remark, however, that the calculations as well as the mentioned generalizations can also be done in the framework of conventional transport theory.[11,12] As pointed out by Lax,[11] in the weak-coupling limit the Kubo formalism leads to the same results as the usual transport theory.

The components of the conductivity tensor in the zero-frequency limit are given by

$$\sigma_{\mu\nu}=V^{-1}\lim_{\varepsilon\to0}\left[\int_0^\infty e^{-\varepsilon t}R_{\mu\nu}(\beta,t)dt\right] , \tag{2.29}$$

where V is the volume of the system, $\beta=(k_BT)^{-1}$, and the correlation function $R_{\mu\nu}(\beta,t)$ is defined as

$$R_{\mu\nu}(\beta,t)=\int_0^\beta\langle J_\nu(-i\hbar\lambda)J_\mu(t)\rangle d\lambda . \tag{2.30}$$

$\langle\cdots\rangle$ denotes $\mathrm{Tr}[\rho\cdots]$ with

$$\rho=e^{-\beta H}/\mathrm{Tr}(e^{-\beta H}) . \tag{2.31}$$

The Hamiltonian H consists of three parts:

$$H=H_h+H_{\mathrm{ph}}+H_I^v . \tag{2.32}$$

H_h is the Hamiltonian of the A^+ and valence-band states of the holes,

$$H_h=\sum_k E(\mathbf{k})a_k^{\dagger}a_k+E^A\sum_j a_j^{\dagger}a_j , \tag{2.33}$$

where $a_k^{\dagger},a_k$ and $a_j^{\dagger},a_j$ are the creation and annihilation operators for a hole with wave vector k in the valence

band and for a hole on an acceptor at site j, respectively. $E(\mathbf{k})$ defines the energy surfaces and $-E^A$ is the binding energy of the A^+ states.

The Hamiltonian of the phonons is written as

$$H_{\rm ph}=\sum_{\mathbf{q},\lambda}\hbar\omega_{\mathbf{q}\lambda}(b^{\dagger}_{\mathbf{q}\lambda}b_{\mathbf{q}\lambda}+\tfrac{1}{2}) , \tag{2.34}$$

and H_I^v is the Hamiltonian (2.2) written in second quantization containing the matrix elements (2.27). In the second quantization the operator of the electric current reads

$$J=e\hbar\sum_{\mathbf{k}}\mathbf{k}a^{\dagger}_k a_k m_h^{-1}(k) , \tag{2.35}$$

where $m_h(k)$ is the mass of a hole in the valence band with wave vector k.

To proceed further, we have to determine the time dependence of the correlation function $R_{\mu\nu}(\beta,t)$. For simplicity, we assume that the system is isotropic, so that the electric field in an arbitrary direction leads to a current in the same direction. Thus, the problem is reduced to one dynamical variable J.

To derive an equation of motion for the correlation function $R(\beta,t)$, we use as starting point the disentangling theorem,[13] written as

$$e^{i(1-P)Lt}=e^{iLt}+\int_0^t d\tau\, e^{iL(t-\tau)}(-iPL)e^{i(1-P)L\tau} , \tag{2.36}$$

with the Liouville operator L defined as

$$iL\,A=(i\hbar)^{-1}[A,H] . \tag{2.37}$$

We multiply Eq. (2.36) from the right-hand side with $(1-P)\dot{J}(0)$, use the following definition of the projection operator P,

$$P=C^{-1}(\beta)|J\rangle\langle J| , \tag{2.38}$$

with

$$C(\beta)=\langle J|J\rangle , \tag{2.39}$$

and take into account the property[14]

$$\langle J|iLJ\rangle=0 \tag{2.40}$$

of the current operator. Thus, we obtain

$$\dot{J}(t)=-\int_0^t d\tau\,\Phi^*(\tau)J(t-\tau)+e^{i(1-P)Lt}(1-P)\dot{J}(t) , \tag{2.41}$$

where Φ^* is the complex conjugate of

$$\Phi=C^{-i}\langle Le^{i(1-P)L\tau}(1-P)LJ|J\rangle . \tag{2.42}$$

This equation describes the time evolution of the operator J. We use the following definition of the scalar product:

$$\langle A|B\rangle=\beta^{-1}\int_0^{\beta}d\lambda\langle e^{\lambda H}A^*e^{-\lambda H}B\rangle . \tag{2.43}$$

Inserting (2.41) in the scalar product describing the correlation function for the correlation between $J(0)$ and $J(t)$,

$$S(t)=\langle J|e^{iLt}|J\rangle , \tag{2.44}$$

we obtain the following equation of motion for the correlation function $S(t)$:

$$\dot{S}(t)=-\int_0^t d\tau\, C^{-1}\langle J|Le^{i(1-P)L\tau}LJ\rangle S(t-\tau) . \tag{2.45}$$

Assuming that Φ decays on a time scale so small that $S(t-\tau)$ is essentially constant on the same scale, we can perform the Markovian approximation in the equation of motion for $S(t)$, which yields

$$\dot{S}(t)=-\int_0^{\infty} d\tau\, C^{-1}\langle LJ|e^{i(1-P)L\tau}LJ\rangle S(t) . \tag{2.46}$$

Additionally, since small interactions between the holes and the phonons are assumed, the Born approximation can be applied. Then Eq. (2.46) is reduced to

$$\dot{S}(t)=-\int_0^{\infty} d\tau\, C^{-1}\langle LJ|e^{i(1-P)(L_h+L_{\rm ph})\tau}LJ\rangle S(t) . \tag{2.47}$$

L_h and $L_{\rm ph}$ are the Liouville operators of the holes and the phonons, respectively. Equation (2.47) has the solution

$$S(t)=e^{-t/\tau} , \tag{2.48}$$

where the inverse relaxation time τ is given by

$$\tau^{-1}=\int_0^{\infty} d\tau\, C^{-1}\langle LJ|e^{i(1-P)(L_h+L_{\rm ph})\tau}LJ\rangle . \tag{2.49}$$

The determination of expression (2.29) is reduced to the calculation of the relaxation time τ. The relaxation time τ is a temperature-dependent quantity. This is a more drastic restriction than in usual transport theory, where the relaxation time is energy dependent.

From the comparison of Eqs. (2.30) and (2.43), we get an equation of motion for the correlation function $R(\beta,t)$ that can be integrated and inserted in Eq. (2.29). Then we end up with the following expression for the electrical conductivity:

$$\sigma(\beta)=V^{-1}\beta\tau(\beta)C(\beta) . \tag{2.50}$$

The operator of the electric current commutes with H_h. Additionally, the commutator of an operator of the hole system with an operator of the phonon system is zero. From these properties it follows

$$(L_h+L_{\rm ph})|J\rangle=0 . \tag{2.51}$$

As an approximation for the case of weak hole-phonon coupling, we perform the scalar product (2.43) only with regard to ρ_0 and H_0. Thereby the density operator is factorized into

$$\rho\approx\rho_0=\rho_h\rho_{\rm ph} , \tag{2.52}$$

with the density operators ρ_h and $\rho_{\rm ph}$ of the uncoupled holes and phonons, respectively, and

$$H_0=H_h+H_{\rm ph} . \tag{2.53}$$

Inserting Eqs. (2.51) and (2.52) into (2.49) and (2.39), we obtain

$$\tau^{-1}(\beta)=C^{-1}(\beta)\int_0^\infty d\tau\langle L_I J|e^{iL_0\tau}L_I J\rangle_{\rho_0,H_0} \tag{2.54}$$

and

$$C(\beta)=\langle J(0)|J(0)\rangle_{\rho_0,H_0}\ , \tag{2.55}$$

where L_0 is the Liouville operator of H_0. Thus, $\tau^{-1}(\beta)$ is of second order and $C(\beta)$ of zeroth order in H_I^v. Further on, we have used the hermiticity of L_0 in the scalar product with respect to ρ_0 and H_0. The calculation of the conductivity is reduced by Eq. (2.50) to the calculation of the relaxation time $\tau(\beta)$ and the quantity $C(\beta)$. Using the commutator relations for Bose and Fermi operators, together with Eqs. (2.35), (2.52), and (2.31), the expression (2.55) for $C(\beta)$ yields

$$C(\beta)=e^2\hbar^2 m_h^{-2}\sum_{kk'}kk'\mathrm{Tr}[\rho_e a_k^\dagger a_k a_{k'}^\dagger a_{k'}]\ . \tag{2.56}$$

Taking into account that $E(k)$ is symmetric in k, going over from summation to integration, and using the density of states

$$D(k)=2V(2\pi)^{-3}\ , \tag{2.57}$$

we end up with

$$C(\beta)=e^2\hbar^2 V m_h^{-2}\pi^{-2}3^{-1}\times\int_0^\infty dk\ k^4(1+e^{\beta E(k)})^{-1}(1+e^{-\beta E(k)})^{-1}\ . \tag{2.58}$$

The integral can be solved by transforming k to $y=\beta E(k)/2$. We get

$$C(\beta)=4Ve^2m^{5/2}\pi^{-2}m_h^{-2}\hbar^{-3}J/[3(\beta C_2)^{5/2}]\ , \tag{2.59}$$

with

$$J=\int_0^\infty dy\ y^{3/2}\cosh^{-2}y=2^{1/2}(1-2^{1/2})\Gamma(\tfrac{5}{2})\zeta(\tfrac{3}{2}) \tag{2.60}$$

in the case of zero stress.

For each M_J^V the form of $E(k)$ has been assumed to be

$$E(k)=C_2\hbar^2k^2/2m+C_4\hbar^4k^4/4m^2\ . \tag{2.61}$$

With these results and with the commutator appearing in Eq. (2.54), which is of the form

$$[H_I^V,J]=\left[\sum_{\substack{q,\lambda,\tau\\k,j\tau}}\left(\frac{\hbar\omega_{q\lambda}}{2Mc_\lambda^2}\right)^{1/2}e\hbar k m_h^{-1}C_{q\lambda}^{M_J^V M_J^A}b_{q\lambda}a_k^\dagger a_j-\text{c.c.}\right]\ , \tag{2.62}$$

an expression for the relaxation time τ can be derived. Going over from summation to integration and using a Debye model for the phonons, we end up with a relaxation time τ of the form

$$\tau^{-1}(\beta)=V^2e^2\hbar\pi^{-3}C^{-1}(\beta)(m_h^{-2}/3)\sum_{M_J^V,M_J^A,\lambda}\int dq\ q^2|M_{M_J^V M_J^A}|^2(e^{\beta\hbar\omega_{q\lambda}}-1)^{-1}(1+e^{\beta E^A})^{-1}\times\int_0^\infty dk\ k^4(1+e^{-\beta E(k)})^{-1}\delta(\hbar\omega_{q\lambda}+E^A-E(k))\ , \tag{2.63}$$

with

$$E^A=-E_0^A\pm\Delta/2\quad\text{for } M_J^A=\begin{cases}\pm\frac{3}{2}\\ \pm\frac{1}{2}\end{cases}\ . \tag{2.64}$$

E_0^A is the binding energy of the A^+ state without stress.

With this we arrive at the following expression for the conductivity $\sigma(\beta)$:

$$\sigma(\beta)\sim\left[\int dq\ q^2\sigma(E_{\mathrm{ph}})(e^{\beta E_{\mathrm{ph}}}-1)^{-1}\right]^{-1}\ . \tag{2.65}$$

The temperature-dependent expression for the conductivity $\sigma(\beta)$ is obtained from the energy-dependent expression $\sigma(E_{\mathrm{ph}})$ with

$$E_{\mathrm{ph}}=\hbar\omega_{q\lambda}\ , \tag{2.66}$$

by integration over the phonon distribution in equilibrium. The *phono*conductivity $\sigma(E_{\mathrm{ph}})$ is defined in Eq. (2.65), which gives

$$\sigma(E_{\mathrm{ph}})\sim\sum_{M_J^V,M_J^A,\lambda}m_h^{-2}\frac{E_{\mathrm{ph}}}{2Mc_\lambda^2}(C_{q\lambda}^{M_J^V M_J^A})^2\times[1+\exp(\beta E^A)]^{-1}\{1+\exp[-\beta(E_{\mathrm{ph}}+E^A)]\}^{-1}k_n^4(|C_2\hbar^2k_n/m+C_4\hbar^4k_n^3/m^2|)^{-1}\ , \tag{2.67}$$

with

$$k_n=(2m\hbar^{-2}\{-C_2+[C_2^2+4C_4(E_{\rm ph}+E^A+\varepsilon/2)]^{1/2}\}(2C_4)^{-1})^{1/2} \quad (2.68)$$

for $M_J^V=\frac{1}{2}$, and

$$k_n=[2m\hbar^{-2}C_2^{-1}(E_{\rm ph}+E^A-\varepsilon/2)]^{1/2},\quad C_4=0 \quad (2.69)$$

for $M_J^V=\frac{3}{2}$.

The effective mass of the hole in a valence-band state $|M_J^V\rangle$ is a function of the k vector of this state,

$$m_h^{-1}=\hbar^{-2}\partial^2 E_{M_J^V}(k)/\partial k^2 . \quad (2.70)$$

The distribution functions in Eq. (2.67) describe the possibility of exciting a hole from the A^+ state into the valence band, taking the occupation of the valence-band states and the A^+ states into account. The influence of applied uniaxial stress enters the expression for the phonoconductivity through its dependence on the structure of the energy surfaces of the valence band, $E_{M_J^V}(k)$. In addition, due to the mixing of the valence-band states with $M_J^V=\pm\frac{1}{2}$, expressions (2.28) are also stress dependent, which is determined by the alternation of the coefficients α_i and β_i with stress.

III. RESULTS

Taking the k^4 correction for the energy surface of the valence band and the valence-band mixing into account, our theoretical model is able to describe qualitatively the behavior of the experimental observations.[15] To measure the phonoconductivity, thin Al junctions, used as tunable phonon generators, are evaporated on one side of the crystal sample. For the measurement of the phonon-induced conductivity, Al contacts are evaporated on the opposite face, which can be illuminated with light for generating a sufficiently large number of carriers, necessary for the production of A^+ states.[15] In contrast to FIR-photoconductivity results,[16] the behavior of the phonoconductivity response is much more complicated, due to the reduced electron-phonon coupling for short-wavelength phonons.

Figures 1 and 2 show the comparison between the experimental measurements of Gross *et al.*[15] and our theoretical calculations in the case of In^+ in Si. The phonoconductivity is plotted as a function of the phonon energy. The calculations have been carried out for various values of uniaxial stress along the [001] direction with the k^4 correction for the energy surface and the valence-band mixing discussed above. The deformation-potential constant of In^+ in Si is smaller than the deformation-potential constant of the valence band. Thus the threshold energy shifts to smaller values under uniaxial stress, and the form factors f_0 and f_2 lead to an increased response signal. The k^4 correction for the energy surface in the case of 328 bars in Fig. 1 causes the stronger decrease of the conductivity with increasing phonon energy, compared to the case of zero stress. Uniaxial stresses of 707 and 1191 bars are strong enough to decouple the valence bands completely. In these two cases no influence of the quartic terms in the wave-vector expansion of the energy surfaces can be seen. It was already pointed out by Suzuki *et al.*[8] that in the case of acceptors in Si the ionization energy calculated by their variational wave function gives, in fact, the correct overall behavior of the experimental tendency, but differs quantitatively by more than 20% from the measured energy values. Therefore, and in order to improve the agreement between the experimental and theoretical results, we have fitted our phonoconductivity response signal by varying the coefficient C_0 of the A^+ wave function. C_0 describes the *s*-like parts of the wave function and is the dominant coefficient. To ensure the normalization of the wave

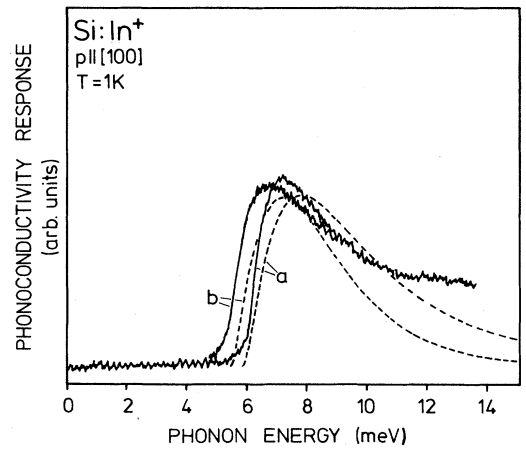

FIG. 1. Phonoconductivity response signal of In^+ in Si for uniaxial stress along [001]. Comparison between experiment (solid line) and theory (dashed line). *a*, 0 bars; *b*, 328 bars. ($r_1=20$ Å, $r_2=13$ Å, $D_u=2.0$ eV, $D_{u'}=3.2$ eV.)

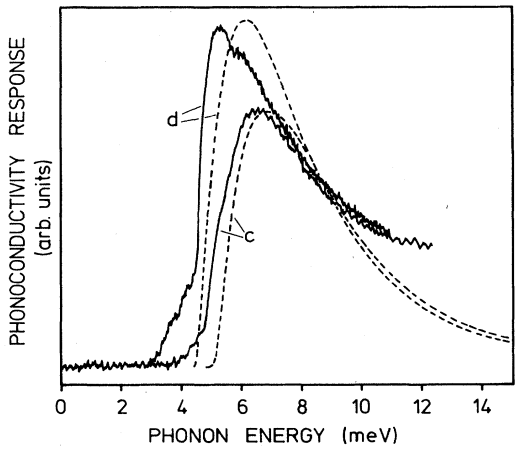

FIG. 2. Phonoconductivity response signal of In^+ in Si for uniaxial stress along [001]. Comparison between experiment (solid line) and theory (dashed line). *c*, 707 bars; *d*, 1191 bars. ($r_1=20$ Å, $r_2=13$ Å, $D_u=2.0$ eV, $D_{u'}=3.2$ eV.)

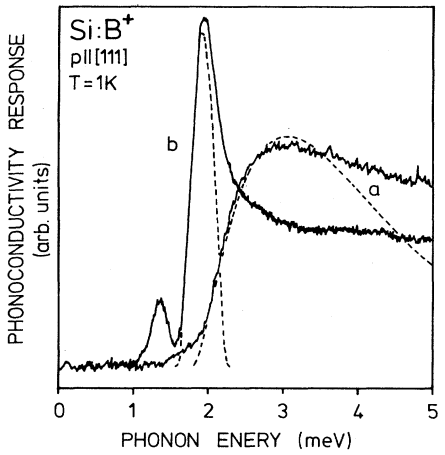

FIG. 3. Phonoconductivity response signal of B^+ in Si for uniaxial stress along [111]. Comparison between experiment (solid line) and theory (dashed line). *a*, 0 bars; *b*, 411 bars. ($r_1=25$ Å, $r_2=16$ Å, $D_u=2.0$ eV, $D_{u'}=3.2$ eV.)

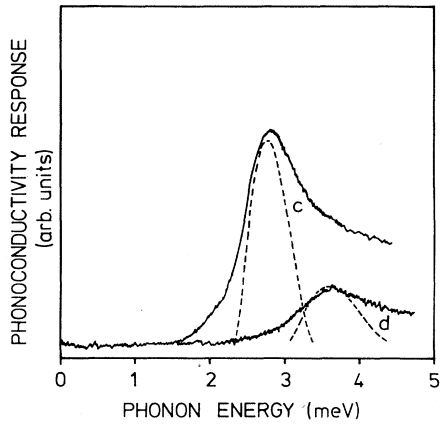

FIG. 4. Phonoconductivity response signal of B^+ in Si for uniaxial stress along [111]. Comparison between experiment (solid line) and theory (dashed line). *c*, 637 bars; *d*, 800 bars. ($r_1=25$ Å, $r_2=16$ Å, $D_u=2.0$ eV, $D_{u'}=3.2$ eV.)

function, we have changed the value of C_2, the amount of which is the greatest of the coefficients describing the *d*-like parts of the wave function. The best agreement was found for a value of C_0 that is 20% below the value determined within the effective-mass approach by the variational calculation of Suzuki *et al.*[8] With this fitting procedure, we obtain the same behavior of the response signal as in the experimental observations of Gross *et al.*[15] The structure in the experimental phonoconductivity signal at phonon energies below the binding energy and the slower decrease of the experimental signal at high phonon energies is due to the fact that the spectrum of the tunnel junction contains not only a monochromatic peak at the phonon energy $eU-2\Delta_G$, where U is the voltage at the tunnel junction and $2\Delta_G$ the energy gap of the junction, but also a precursor at the phonon energy eU and an approximately continuous contribution at the phonon energies below $eU-2\Delta_G$.[17]

The phonoconductivity of B^+ in Si with the k^4 correction and the valence-band mixing is compared with the observed signals in Figs. 3 and 4. Here the direction of uniaxial stress is taken along [111]. The decrease of the phonoconductivity signal with low stress is caused by the k^4 correction and the splitting of the B^+ and the valence-band states with applied stress. This changes the occupation of the B^+ states and shifts a part of the transition to higher energies with decreased form factors. The sharp line appearing when the stress is increased is caused by two effects. First, with the onset of decoupling of the valence bands, the effective mass of the mobile charge carrier is reduced and leads to an increased conductivity. Second, the k^4 correction has the opposite effect. It increases the effective mass at higher phonon energies and suppresses the conductivity signal. With higher values of applied stress, the signal is shifted to higher energies. This is a consequence of the different deformation-potential constants of the valence band and the A^+ state. When the stress is strong enough to decouple the valence bands completely, the k^4 correction can be neglected. This leads to a signal as in the case of 800 bars in Fig. 4. Again, with the same coefficients C_i for the wave function as in the case of In^+ we obtain good qualitative agreement with the measurements of Gross *et al.*[15] As in the case of In^+, the structure of the experimental signal at phonon energies below the binding energy of the A^+ state and the slow decrease of the experimental signal at high phonon energies is due to the spectrum of the tunnel junction.

The phonoconductivity response signal is very sensitive to the power of k in expression (2.67). Since the second-order correction of the energy surface (2.17) is only valid in the region near $k=0$, one does not know the correct shape of the valence band for larger values of the wave vector k. A small correction of the wave-vector expansion of the energy surface can have striking effects on the phonoconductivity. This can be seen in Figs. 3 and 4, where the k^4 correction is important in order to explain the experimental observations.

To summarize, we have shown that the phonoionization of A^+ states in Si has a strong dependence on the phonon energy due to the reduced electron-phonon coupling of short-wavelength phonons. Further, our calculations demonstrate that stress tuning of the valence-band structure (decoupling of degenerate bands and valence-band mixing) has striking effects on the phonoconductivity response signal, as is also observed experimentally.

ACKNOWLEDGMENTS

We gratefully acknowledge valuable discussions with P. Gross and K. Lassmann and we would like especially to thank P. Gross, who has placed his measurements at our disposal. We want to thank the Deutsche Forschungsgemeinschaft (DFG) for financial support.

[1]W. Burger and K. Lassmann, Phys. Rev. Lett. **53**, 2035 (1984).
[2]M. Taniguchi and S. Narita, Solid State Commun, **20**, 131 (1976).
[3]S. Narita, T. Shinbashi, and M. Kobayashi, J. Phys. Soc. Jpn. **51**, 2186 (1982).
[4]W. Burger and K. Lassmann, Phys. Rev. B **33**, 5868 (1986).
[5]R. Kubo, J. Phys. Soc. Jpn. **12**, 570 (1957).
[6]M. Mori, Prog. Theor. Phys. **33**, 423 (1965).
[7]T. Fjeldly, T. Ishiguro, and C. Elbaum, Phys. Rev. B **7**, 1392 (1973).
[8]K. Suzuki, M. Okazaki, and H. Hasegawa, J. Phys. Soc. Jpn. **19**, 930 (1964).
[9]H. Hasegawa, Phys. Rev. **102**, 1029 (1963).
[10]J. C. Hensel and G. Feher, Phys. Rev. **129**, 1041 (1963).
[11]M. Lax, Phys. Rev. **109**, 1921 (1958).
[12]L. Van Hove, Physica **21**, 517 (1955).
[13]R. P. Feynman, Phys. Rev. **84**, 108 (1951).
[14]B. J. Berne and G. D. Harp, in *On the Calculation of Time Correlation Functions,* Vol. 17 of *Advances in Chemical Physics,* edited by J. Prigogine and S. A. Rice (Wiley-Interscience, New York, 1970).
[15]P. Gross, M. Gienger, and K. Lassmann, Jpn. J. Appl. Phys. (Suppl. 3) **26**, 673 (1987).
[16]N. Sugimoto, S. Narita, M. Taniguchi, and M. Kobayashi, Solid State Commun. **30**, 395 (1979).
[17]W. Burger, Ph.D. thesis, University of Stuttgart, 1986.